Journal of Crystal Growth 474 (2017) 24–30

Contents lists available at ScienceDirect

Journal of Crystal Growth

journal homepage: www.elsevier.com/locate/jcrysgro

Crystal front shape control by use of an additional heater in a Czochralski sapphire single crystal growth system

Min-Jae Hur, Xue-Feng Han, Ho-Gil Choi, Kyung-Woo Yi*

Department of Materials Science and Engineering, Seoul National University, Seoul 151–744, South Korea

ARTICLE INFO

Communicated by Dr. Francois Dupret

Keywords:
A2. Czochralski method
B1. Sapphire
A2. Growth from melt
A2. Single crystal growth

ABSTRACT

The quality of sapphire single crystals used as substrates for LED production is largely influenced by two defects: dislocation density and bubbles trapped in the crystal. In particular, the dislocation density has a higher value in sapphire grown by the Czochralski (CZ) method than by other methods. In the present study, we predict a decreased value for the convexity and thermal gradient at the crystal front (CF) through the use of an additional heater in an induction-heated CZ system. In addition, we develop a solute concentration model by which the location of bubble formation in CZ growth is calculated, and the results are compared with experimental results. We further calculate the location of bubble entrapment corresponding with the use of an additional heater. We find that sapphire crystal growth with an additional heater yields a decreased thermal gradient at the CF, together with decreased CF convexity, improved energy efficiency, and improvements in terms of bubble formation location.

1. Introduction

Recent increases in demand for LED's has led to a corresponding rise in the demand for materials used in LED production. Various materials may be employed as the substrate for LED's, such as sapphire, Si, SiC and GaN, but currently the most commonly used is sapphire single crystal. Sapphire single crystals may be obtained with good throughput through the CZ method with growth in the c-axis direction. However, sapphire c-axis growth using the CZ method leads to a high dislocation density within crystal, which is 20–100 times higher than for crystals grown by the Kyropoulos (KY) method. High dislocation densities can lead to substrate fracture during GaN deposition or diminished LED efficiency [1,2].

Bubbles in sapphire single crystals are, along with dislocations, an important defect. Oversaturated O or CO in the melt can be trapped as bubbles at the crystal front(CF) during crystal growth and lead to diminished throughput. Studies regarding this issue have in the past mostly dealt with sapphire grown using the EFG method [3–7]. According to results of previous studies [3–6], bubble entrapment in the crystal is unavoidable during sapphire bulk crystal growth, and the only solution is to control the system in such a way that the bubbles are formed not at the crystal center but at the periphery. As the location of bubble entrapment is governed by the melt flow, controlling the melt flow is an essential aspect in determining sapphire single crystal quality.

In the present study we create a model of a CZ system in which a 4 in. boule is grown with induction heating, and the results are compared against experimentally measured values to evaluate the model effectiveness. We implemented additional heaters to decrease thermal gradient deviations at the CF and flatten the CF shape in order to decrease the dislocation density in the crystal, and obtained corresponding calculated results. We also calculated where bubbles will be trapped in the crystal as a result of the melt flow direction being altered by the additional heater.

2. Global modeling of CZ system

2.1. Numerical model

In this study, we developed a 2D axis-symmetric global simulation model of a 4 in. boule. As the sapphire single crystal growth is a very slow process, we assume quasi-steady state conditions in the global model [8]. The physical properties of sapphire melt and crystal are given in Table 1 [9,10].

The model takes into account different physical phenomena such as flow, heat transfer, magnetic effects, radiation and turbulence. We use the Sn discrete ordinate method for radiation calculation and the standard k-ε model (Launder and Spalding model) for turbulence [11,12].

* Corresponding author.
E-mail address: yikw@snu.ac.kr (K.-W. Yi).

http://dx.doi.org/10.1016/j.jcrysgro.2016.12.078
Received 16 December 2016; Received in revised form 19 December 2016; Accepted 21 December 2016
Available online 27 December 2016

Table 1
Physical properties used in this study.

Description	Value (unit)
Melt viscosity	0.057 (Pa s) [7]
Melt density	3030 (Kg/m^3) (at 2327 K) [7]
Melt thermal conductivity	2.02 (W/m k) (at 2027 K) [7]
Melt heat capacity	1260 (J/Kg K) [7]
Melt emissivity	0.33 [8]
Crystal density	3970 (Kg/m^3) (at 2327 K) [7]
Crystal thermal conductivity	5.6 (W/m K) (at 1700 K) [7]
Crystal heat capacity	1313 (J/Kg K)(at 1700 K) [7]
Crystal emissivity	0.869 [8]
Solubility of melt	7.8×10^{-10} (kmol/m^3) (estimated)
Solubility of crystal	7.8×11^{-10} (kmol/m^3) (estimated)
Diffusivity of oxygen in melt	1.5×10^{-9} (m^2/s) [7]

2.2. Tracking of the crystal growth interface

The global model reflects the solidification of the melt and the melting of the solid by varying the viscosity based on a melting temperature of Tm=2327 K. Each cell is assigned the viscosity, thermal conductivity, heat capacity, and radiation properties of the melt for a temperature higher than Tm, and a viscosity of 20 (kg/m s) and the properties of the sapphire crystal at temperatures below Tm. We do not take into account latent heat in this model. When the growth rate is 1 mm/h, the ratio of (latent heat)/(conduction heat released through the crystal) is 0.05. So ignoring the latent heat can be acceptable, and even disregarding radiation heat release through the crystal. This method allows for stable calculations as no adjustment of the grid is required to reflect changes in the CF shape [12].

3. Global model results and analysis

3.1. Model verification through comparison with experimental results

In the present study we choose to compare the CF shape for calculated and experimentally measured results in order to evaluate the model effectiveness. This method is relatively costly, but it is judged to be the most appropriate in evaluating the model, as it provides direct confirmation of whether the CF shape, which is of primary importance in this study, is properly reflected in the model. To verify the accuracy of the model, we performed comparisons for two stages, the shouldering stage and the body growth stage. Calculated results for both the shouldering stage and body growth stage are in very good agreement with experimental results (Fig. 1). This demonstrates that the model used in the present study accurately reflects the actual system.

3.2. Decreased temperature gradient at CF by use of additional heater

Sapphire growth in the c-axis direction results in a high dislocation density within the crystal, which is a leading cause of diminished LED efficiency. Therefore, the production of higher quality LEDs requires achieving lower dislocation density in the sapphire crystal. There are many causes of dislocation formation during sapphire single crystal growth, but one of the most important is dislocation formation by thermal stress near the CF. Sapphire has a very narrow plastic zone near the melting temperature, so that apart from dislocations originating from the seed, the ones formed during crystal growth are mostly caused by thermal stress in a narrow range near the CF directly after crystallization [9]. Therefore, in order to decrease dislocation density within the crystal, it is important to decrease thermal stress at the CF. The present study explores a way to decrease thermal stress at the CF by employing an additional heater.

In most cases, sapphire growth by the CZ method involves a shape of the CF extending below the melt as in Fig. 1.b. The temperature gradient depends on the location at the CF, which results in values of 10–32 K/cm (Fig. 2). Compared to KY method sapphire growth, which results in a CF temperature gradient of 0–5 K/cm [13], which are very high values. Additionally, existing growth conditions using the CZ method result in high values not only for the absolute value of the temperature gradient, but also for the deviation of the temperature gradient in the radial direction at the CF. The deviation of temperature gradient can lead to shear stress within the crystal because of the varying thermal expansion between radial locations [12]. In short, CZ method growth conditions, in comparison with KY method, result in higher thermal gradient absolute values and deviation according to location, so that a larger thermal stress is unavoidable. The larger temperature gradient for the CZ method can be attributed to a hot-zone structure which results in a larger temperature variation in the vertical direction. Therefore, the production of higher quality crystals will require an improved control of the hot-zone temperature distribution to decrease the thermal gradient at the CF as well as to minimize the deviation according to location.

The most important factor to influence temperature gradients at the CF during sapphire growth is the melt flow. Because molten sapphire has a relatively high Prandtl number, convection has a major impact on the temperature distribution in the melt. The Prandtl number can be defined as follows:

$$\mathrm{Pr} = \frac{v}{\alpha} = \frac{\text{viscousdiffusionrate}}{\text{thermaldiffusionrate}} = \frac{C_P \mu}{k}$$

A higher Prandtl number indicates a larger heat transfer by convection than by conduction within the fluid. The sapphire melt has a Prandtl number of 35, much higher than the values of 7 for water, or 0.009 for the silicon melt [12,14]. Therefore, in order to change the temperature gradient at the CF, the melt flow must first be changed.

The generation of heat during induction heating mostly takes place at the crucible side, as shown in Fig. 3.a. In the presence of induction heating only, heat is generated from the side to create natural convection as shown in Fig. 3.b. With melt convection formed as in Fig. 3.b, the melt heated to a high temperature flows from the crystal periphery to the center, and is slowly cooled, so that a relatively higher temperature gradient is found at the crystal periphery. Fig. 2 graphically shows differences in the temperature gradient depending on the location on the CF for the cases of induction heating only and the application of an additional heater. By altering the hot-zone temperature distribution and the melt convection direction by use of this additional heater, the temperature gradient absolute value is lowered and the location dependent deviation is also greatly reduced. Therefore, the use of an additional heater lowers the thermal stress in the plastic zone, and crystal growth under such conditions can be predicted to result in a lower dislocation density than before. In general, Fig. 4 shows the CF shape change with induction and additional heating powers. Induction heating power should be decreased to fit the triple-point (crystal-melt-gas) when using an additional heater.

3.3. Decreased CF convexity by use of additional heater

Much like the thermal gradient at the CF, the flatness of the CF shape during crystal growth is also of great importance in determining the crystal quality. In short, a flatter CF shape results in improved crystal quality [15,16]. To evaluate the flatness, we implement the concept of convexity as outlined by Chen et al. [15]. The convexity refers to the difference in height between the highest and lowest points of the crystal-melt interface within the melt.

Several studies in the past have suggested to raise the crystal rotation rate in order to alter the melt flow direction or the CF shape [17–20]. Generally, an increase of the crystal rotation rate results in a stronger forced convection. The centrifugal force of forced convection forms a flow from the crystal center to the outer regions, which results in decreased convexity.

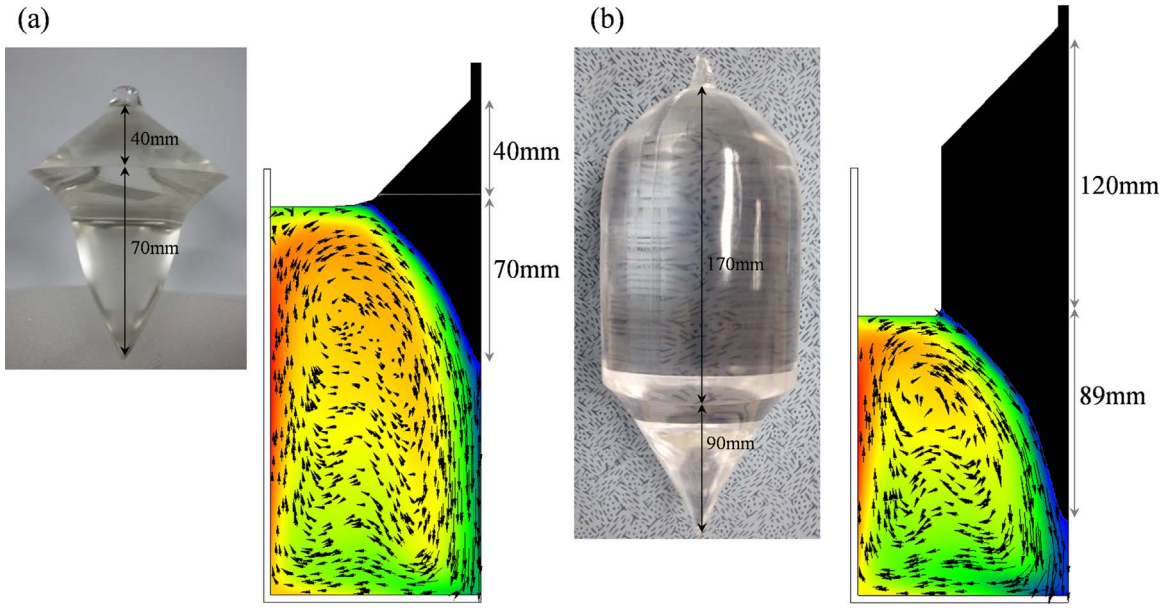

Fig. 1. Comparison of the CF shape for calculated and experimentally measured results. (a) Shouldering stage and (b) body growth stage.

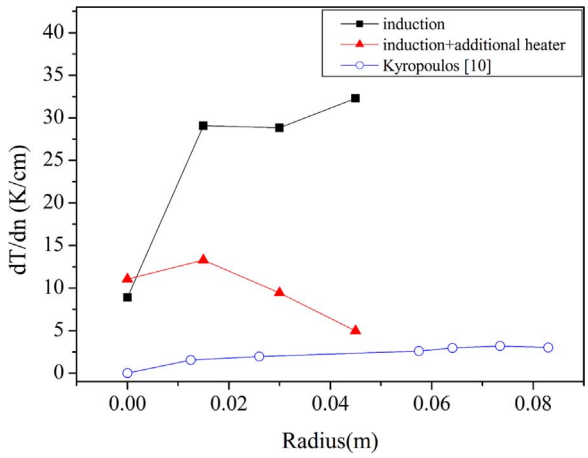

Fig. 2. Thermal gradient variation with radial position at CF.

In the present study, we employ an additional heater instead of forced convection to create a reverse direction natural convection and thereby alter the CF shape and temperature distribution. The advantage of this method is that convexity can be decreased even at lower crystal rotation rates so that more stable growth is made possible, which is predicted to be of even greater advantage in the future when the diameter of the grown crystal is increased. The additional heater was simulated in the numerical model by applying heat flux at the bottom of the crucible, and the results of the simulation are shown in Fig. 3.c. The heat provided by the additional heater creates a force which lifts the melt from the bottom of the crucible to the crystal, resulting in a natural convection which is opposite to that which was observed before, and thereby creates a flat CF shape.

4. Solute concentration modeling for CZ system

Sapphire growth for LED substrates currently employs various melt growth methods. Sapphire which is produced using such methods will have bubbles (voids) in the crystals unless specific growth conditions are met, which can be detrimental to crystal quality and throughput [5,7]. Regarding the mechanism by which bubbles are formed in the crystal, various studies have been presented dealing with sapphire growth through the EFG method. The solute segregation theory as presented in [5] is in good agreement with results obtained experimentally from EFG systems. The solute segregation theory proposes that differences in oxygen (or carbon monoxide) solubility between the melt and crystal lead to segregation at the CF, and with continued occurrence of this phenomenon along with melt flow, solute pile-up arises at specific locations. At locations where the pile-up creates an oversaturation of solute, bubble nuclei are formed. If the bubble grows past a certain size, it is trapped within the crystal [5]. Based on the solute segregation theory, in the present study we developed a solute concentration model which predicts bubble location and is applicable at the CF with the CZ method. According to [5], an assumption was made that in all cases, the solubility limit of the gas in the liquid was reached, and that it did not depend significantly on the various growth parameters. The results from the model were compared with experimentally obtained results.

Fig. 5 shows the structure and numerical results of the solute concentration model. This model only considers solute transport, diffusion and segregation without including bubble nucleation, growth and incorporation into the crystal. Since bubble formation is a phenomenon which occurs within the melt, the model geometry was created based on a CF shape obtained through calculated and experimentally measured results, while the bottom, side wall, and free surface were given temperature conditions taken from the global model. The solute segregation phenomenon caused by solubility differences between the crystal and melt during the crystal growth process is simulated in the model by applying oxygen flux at the CF (as the equipment for experimentation and modeling in the present study does not contain materials with carbon content, calculations are performed for oxygen, rather than carbon monoxide).

In order to calculate the oxygen solute flux at the CF, our approach is to determine the melt and crystal oxygen solubility (C_L,C_S) and segregation coefficient ($k = C_S/C_L$). A value of 0.1 is taken from a separate study for the segregation coefficient [21]. However, as there are no known values for C_L or C_S, the values are calculated using measured results of bubble amounts trapped in crystals grown by the EFG method. When oxygen supersaturated melt moves to the free surface, it forms an equilibrium with the atmosphere and has a value of C_L. However, the free surface is very narrow and the melt flow is weak for the EFG method, so that oxygen out-diffusion through the free surface is negligible. Therefore, it can be assumed that all bubbles trapped into the crystal, where they are found, are due to the difference between C_L and C_S. According to experimental results, the amount of

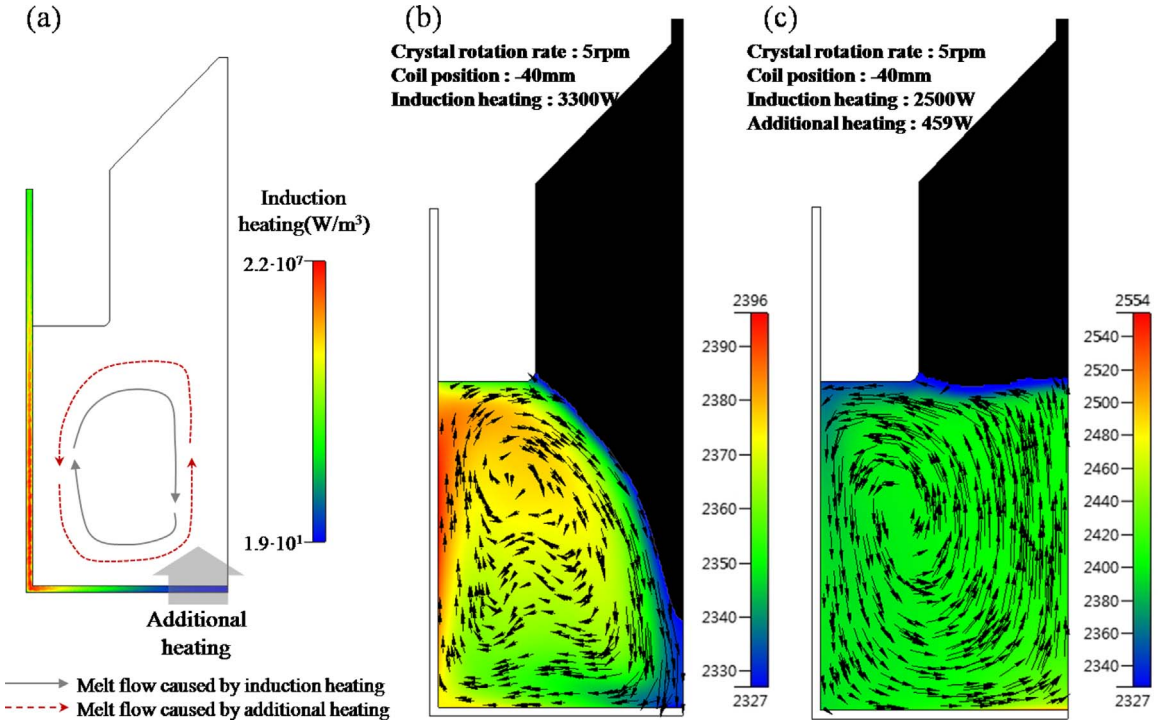

Fig. 3. (a) Heating region by induction heating and additional heater position. (b) Melt flow pattern and CF shape in the presence of induction heating only. (c) Melt flow pattern and CF shape in the presence of induction heating and additional heating.

bubbles trapped in crystals grown by the EFG method has a fixed value of 7.0×10^{-10} kmol/m^3 regardless of the growth conditions [5]. This results in the equations below:

$$C_L - C_S = 7 \times 10^{-10}$$
$$C_S = k \times C_L$$

$$\therefore C_L = \frac{7\times10^{-10}}{0.9} = 7.778 \times 10^{-10}\text{kmol/m}^3$$
$$C_S = 7.778 \times 10^{-11}\text{kmol/m}^3$$

Calculating oxygen flux at the CF from the result above gives

$$A = \pi\ r^2,\ V = A\ v$$
$$\text{oxygenfluxatCF} = \frac{C_L(1-k)\ V}{A} = 1.95 \times 10^{-16}\text{kmol/m}^2\text{s}$$

with A=vertical section area of crystal, V=volume of growing crystal per second (m^3/s), v=growth rate(1 mm/h).

The boundary conditions of our solute concentration model are obtained as follows from the above discussion: in most cases in CZ, unlike in EFG, the CF shape is not flat, and instead shows a curved

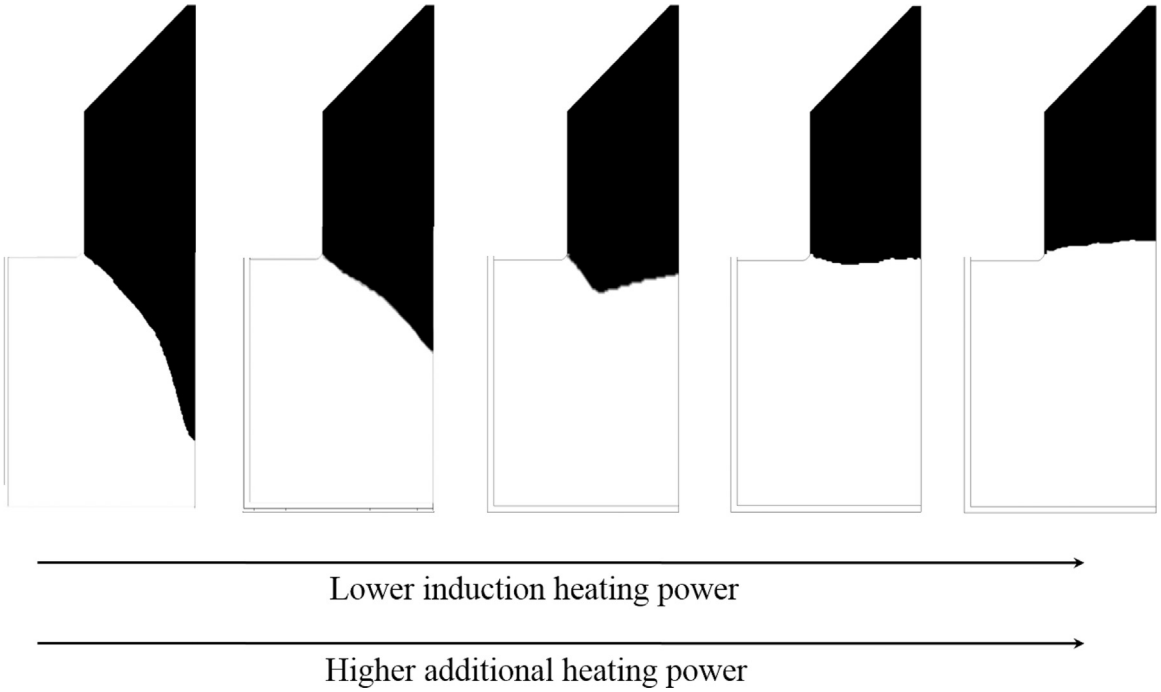

Fig. 4. CF shape change with induction and additional heating powers.

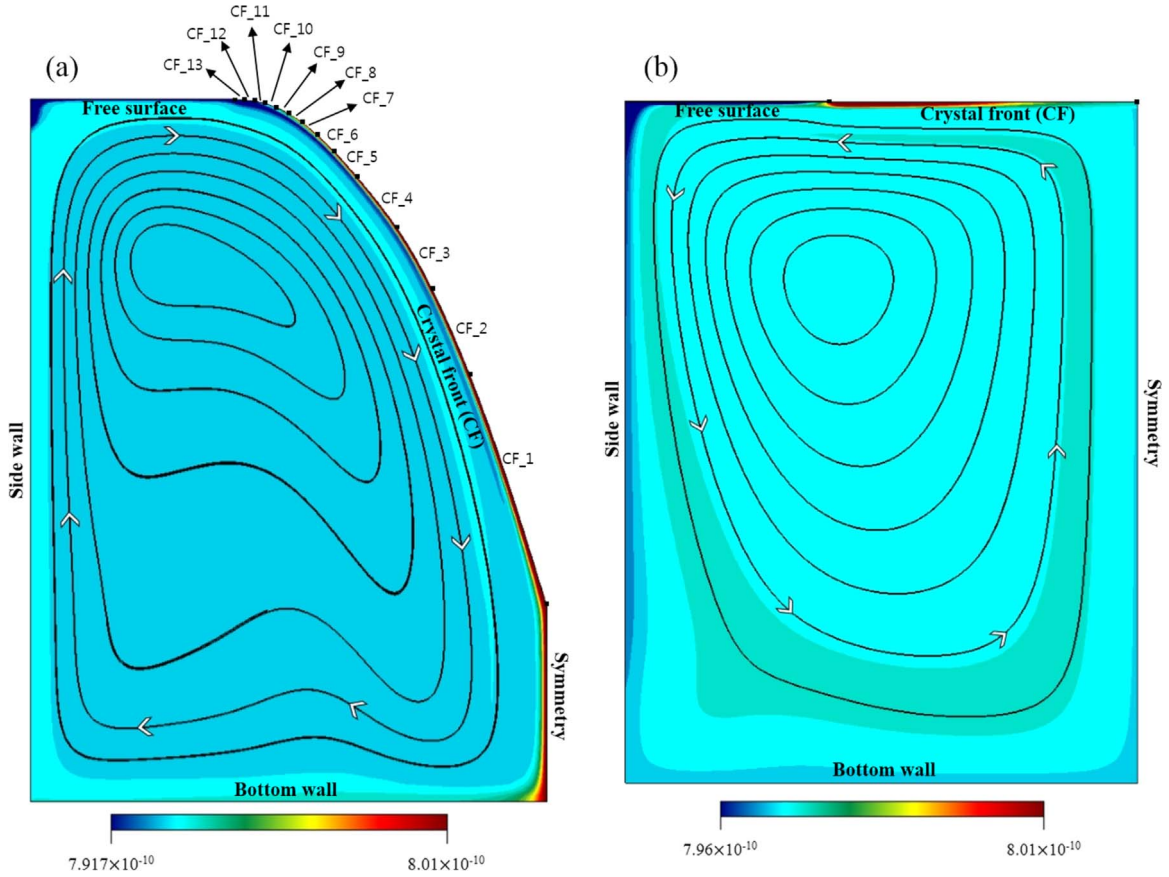

Fig. 5. Boundary conditions and numerical results (melt flow and oxygen concentration distribution) of solute concentration model: (a) Curved CF model and (b) flat CF model. The oxygen flux across the CF segments is as follows: CF_1–0.612, CF_2–0.769, CF_3–0.952, CF_4–1.190, CF_5–1.291, CF_6–1.393, CF_7–1.517, CF_8–1.633, CF_9–1.735, CF_10–1.835, CF_11–1.911, CF_12–1.935, CF_13–1.943 (x 10^{-16}kmol/m^2s).

shape which extends into the melt (Fig. 5.a). As the crystal growth rate per unit area differs depending on the CF slope, the CF must be divided into multiple sectors depending on the slope where an appropriate corresponding oxygen flux is designated. As shown in Fig. 5.b, a flat CF due to the use of an additional heater negates the flux value differences for each section.

The initial conditions for the solute concentration model are taken from steady state results of calculations taking into account only flow and heat, without oxygen concentration. The initial oxygen concentration of the melt is set as the saturated concentration (C_L) [5]. Oxygen flux at the CF continuously and gradually raises the melt oxygen concentration, and as supersaturated melt reaches equilibrium at the free surface with the saturated concentration, the boundary condition for the free surface is set as the C_L. In the present study we performed both steady state and transient calculations for curved and flat CF geometries, with transient calculations performed for a period of 24 h following the initial conditions. Boundary layer effects were considered.

5. Solute concentration model results and analysis

5.1. Verification of solute concentration model by comparison with experimental results

Fig. 5 shows the flow results of the solute concentration model as well as the overall oxygen concentration distribution in the melt. Comparing Fig. 5.a and Fig. 5.b, the solute pile-up location is governed by the melt convection direction, and so the melt which has a decreased oxygen concentration after passing the free surface is found to regain a higher oxygen concentration near the CF.

Of the total concentration distribution, the concentration of the CF part is shown graphically in Fig. 6.a. The solid line shows results for the curved CF and the dashed line corresponds with results for the flat CF. Steady state results are shown in red and blue, respectively, and transient results are given by 1 h increments from hour 1 to hour 24. The oxygen concentration for the melt is given an initial condition of C_L and as calculation progresses, oxygen flux at the CF continuously raises the oxygen concentration. For the curved CF model, the melt flow is directed from the free surface to the crystal so that melt with a concentration lowered to C_L at the free surface passes by the CF. As a result, the oxygen concentration is lower near the free surface but rises with closer proximity to the crystal center due to pile-up phenomena, and the region of highest oxygen concentration is formed near the crystal center. This trend is also found in transient results.

Interpreting curved CF results based on the solute segregation theory, bubbles are formed where solute supersaturation is the highest, i.e. in at the crystal center region and are trapped in the crystal. Fig. 7 shows photographs of a crystal grown in conditions identical to the curved CF model as well as bubbles within the crystal. Experimental results also reveal bubbles having formed and been trapped near the crystal center. We can therefore conclude that the numerical model based on the solute segregation theory can explain experimental results for the CZ method.

5.2. Calculation of bubble entrapment location in crystal growth using additional heater

As the solute concentration model (curved CF model) is in good agreement with experimental results, we applied it to calculate bubble formation locations in crystal growth using an additional heater (flat CF model). Crystal growth with an additional heater involves a melt

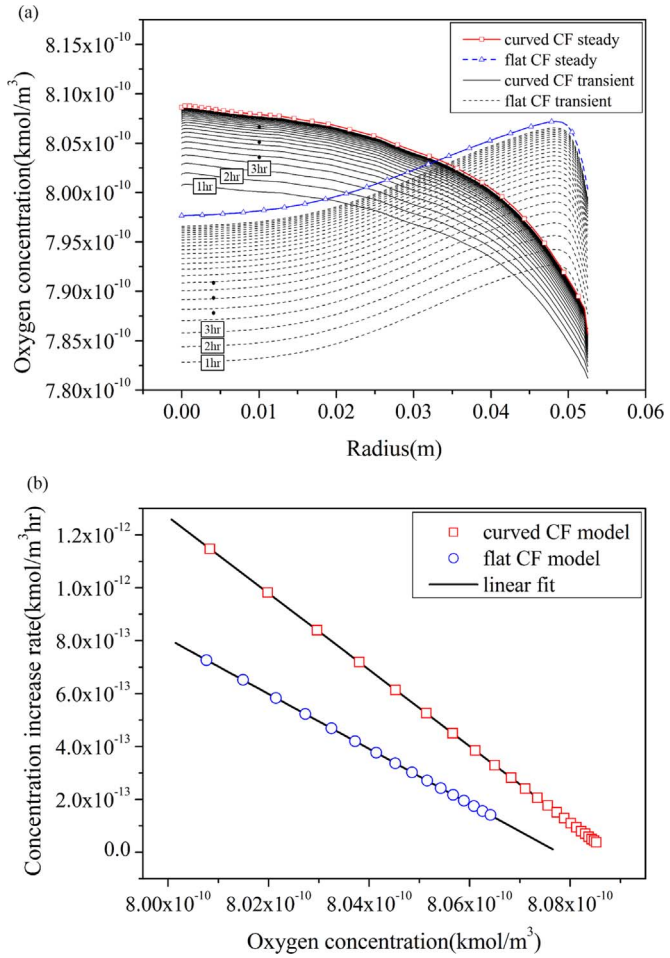

Fig. 6. Numerical results comparison of curved CF model with flat CF model. (a) Oxygen concentration distribution at CF and (b) Concentration increase rate at solute pile-up region according to concentration at solute pile-up region.

convection direction opposite to that of previous CZ growth, and its CF shape is also flat. As such, a corresponding model is shown in Fig. 5.b, and the boundary conditions are taken from temperature results obtained from the global model.

The use of an additional heater results in melt convection directed from the CF center to the free surface, so that solute pile-up occurs at the crystal periphery. Bubble nucleation occurs when the oxygen concentration exceeds a certain value, and the bubbles are trapped in the crystal after growth. The bubble growth process was not calculated in the present study, but it was possible to predict the degree of bubble entrapment by analyzing the rate at which oxygen concentration increases in the region of solute pile-up.

Fig. 6.b shows the rate of oxygen concentration increase over time in the region of solute pile up (curved CF: at radius 0.5 mm, flat CF: at 48.51 mm) from the transient results in Fig. 6.a. For example, when the maximum oxygen concentration at the CF is 8.038×10^{-10} (kmol/m^3), the maximum oxygen concentration increases at a rate of 7.2×10^{-13} (kmol/m^3h) for the curved CF, and 4.1×10^{-13} (kmol/m^3 h) for the flat CF. A trend is observed in which a higher oxygen concentration brings out-diffusion at the free surface and flux at the CF closer to equilibrium, so that the pile-up rate is decreased. Also, for a given oxygen concentration at a pile-up location, the concentration increase rate is lower for the flat CF than for the curved CF. A lower rate of concentration increase indicates a smaller bubble size or a lower frequency of its entrapment. Hence, if additional heaters are used to change the melt convection direction and flatten the CF shape, the intervals between bubbles are lengthened or the bubble sizes are decreased compared to a curved CF. In addition, the location of the bubbles is moved from the crystal center to the crystal periphery.

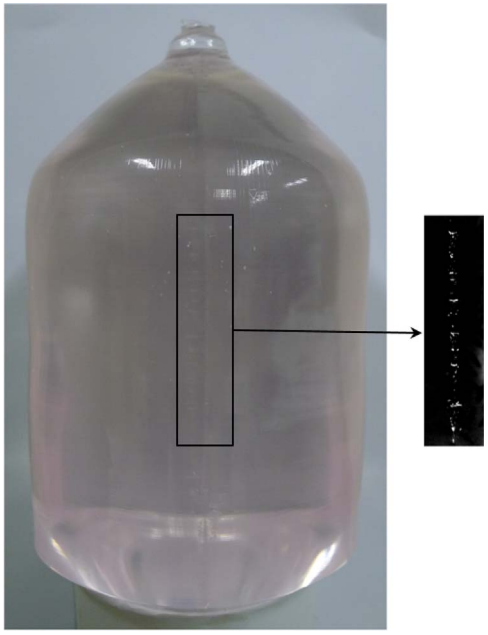

Fig. 7. A crystal grown in conditions identical to curved CF model and bubbles therein.

Bubbles trapped at the outer edges of the crystal can be eliminated through polishing or coring and therefore this is expected to be of great importance in improving crystal quality.

6. Conclusion

In the present study, we created a numerical model of an induction-heated CZ sapphire growth system, and verified the model through comparison with experimentally obtained results. Moreover, we calculated changes in the CF shape corresponding with the use of an additional heater. Changes in the CF shape with the use of an additional heater were found to occur through changes in the melt flow direction and hot-zone temperature distribution, and in comparison with previous crystal growth methods, this was found to result in lower absolute values for the thermal gradient at the CF as well as smaller deviations according to location.

Regarding the formation of bubbles, a major defect in sapphire growth, we developed a solute concentration model through the solute segregation theory, mostly investigated in relation to the EFG method. The model is found to be applicable also to the CZ method despite very different CF shapes and melt velocities. The numerical model results were found to be in good agreement with experimental results in terms of the locations of bubble entrapment. The model was used to predict that under growth conditions involving an additional heater, bubbles would be trapped at the crystal peripheral edges. This is expected to be of great value in improving crystal quality. In conclusion, the advantages of an additional heater in crystal growth can be summarized as follows:

1. Decreased thermal gradient (for both absolute value and deviations between different locations)
2. Decreased convexity (flat CF shape)
3. Decreased energy needed for crystal growth (Numerically, approximately 10%)
4. Bubble formation location moved to outer edges of crystal.

We have no experimental result with an additional heater. Therefore the results of this additional heater method have to be validated by appropriate experiments.

References

[1] L. Zhang, et al., Tridimensional morphology and kinetics of etch pit on the {0 0 0 1} plane of sapphire crystal, J. Solid State Chem. 192 (0) (2012) 60–67.
[2] F.J. Bruni, C.M. Liu, J. Stone-Sundberg, Will Czochralski growth of sapphire once again Prevail?, Acta Phys. Pol. A 124 (2) (2013) 213–218.
[3] O. Bunoiu, et al., Fluid flow and solute segregation in EFG crystal growth process, J. Cryst. Growth 275 (1–2) (2005) e799–e805.
[4] O. Bunoiu, et al., Thermodynamic analyses of gases formed during the EFG sapphire growth process, J. Cryst. Growth 275 (1–2) (2005) e1707–e1713.
[5] O.M. Bunoiu, T. Duffar, I. Nicoara, Gas bubbles in shaped sapphire, Prog. Cryst. Growth Charact. Mater. 56 (3–4) (2010) 123–145.
[6] I. Nicoara, O.M. Bunoiu, D. Vizman, Voids engulfment in shaped sapphire crystals, J. Cryst. Growth 287 (2) (2006) 291–295.
[7] H. Li., et al., Bubbles defects distribution in sapphire bulk crystals grown by Czochralski technique, Opt. Mater. (2013).
[8] J.J. Derby, R.A.B, On the quasi-steady-state assumption in modeing Czochralski crystal growth, J. Cryst. Growth 87 (1988) 251.
[9] Elena R. Dobrovinskaya, L.A.L. Valerian Pishchik, Sapphire Material, Manufacturing, Applications 170–176, Springer, New York, 2010, p. 288.
[10] W.J. Lee, et al., Effect of crucible geometry on melt convection and interface shape during Kyropoulos growth of sapphire single crystal, J. Cryst. Growth 324 (1) (2011) 248–254.
[11] CFD-ACE+ v.2011.0 Modules Manual.
[12] M.-J. Hur, et al., The influence of crucible and crystal rotation on the sapphire single crystal growth interface shape in a resistance heated Czochralski system, J. Cryst. Growth 385 (0) (2014) 22–27.
[13] S.E. Demina, et al., Use of numerical simulation for growing high-quality sapphire crystals by the Kyropoulos method, J. Cryst. Growth 310 (7–9) (2008) 1443–1447.
[14] Chong E. Chang, William R. Wilcox, Robert A. Lefever, Thermocapillary convection in floating zone melting: influence of zone geometry and prandtl number at zero gravity, Mater. Res. Bull. 14 (4) (1979) 527–536.
[15] J.-C. Chen, C.-W. Lu, Influence of the crucible geometry on the shape of the melt–crystal interface during growth of sapphire crystal using a heat exchanger method, J. Cryst. Growth 266 (1–3) (2004) 239–245.
[16] H.S. Fang, J. Tian, S. Wang, Y. Long, M.J. Zhang, C.J. Zhao, Numerical optimization of Czochralski sapphire single crystal growth using orthogonal design method, Cryst. Res. Technol. (2014).
[17] O. Asadi Noghabi, M. M'Hamdi, M. Jomâa, Effect of crystal and crucible rotations on the interface shape of Czochralski grown silicon single crystals, J. Cryst. Growth 318 (1) (2011) 173–177.
[18] K.K. Lijun Liu, Effects of crystal rotation rate on the melt–crystal interface of a CZ-Si crystal growth in a transverse magnetic field, J. Cryst. Growth 310 (2) (2008) 306–312.
[19] Y.-R. Li, et al., Global analysis of a small Czochralski furnace with rotating crystal and crucible, J. Cryst. Growth 255 (1–2) (2003) 81–92.
[20] U. Rehse, et al., A numerical investigation of the effects of iso- and counter-rotation on the shape of the VCz growth interface, J. Cryst. Growth 230 (1–2) (2001) 143–147.
[21] O. Bunoiu, et al., Numerical simulation of the flow field and solute segregation in edge-defined film-fed growth, Cryst. Res. Technol. 36 (7) (2001) 707–717.